

“SWASTHA-SHWASA”: UTILITY OF DEEP LEARNING FOR DIAGNOSIS OF COMMON LUNG PATHOLOGIES FROM CHEST X-RAYS

Aishwarya N¹, Veena M B², Dr. YashasUllas L³ and Dr. RajsriThuthikadu Rajasekaran⁴

¹Student, M.Tech Electronics, B M S College of Engineering

²Senior Member IEEE, Associate Professor, B M S College of Engineering

³Diagnostic Radiologist, Sri Devaraj Urs Academy of Higher Education and Research Centre

⁴Evidence Scientist, Department of Community Medicine, Evidencian Research Associates

¹aishwaryan.le119@bmsce.ac.in, ²veenamb.ece@bmsce.ac.in, ³dryashasullas@gmail.com and

⁴rsri34@gmail.com

ABSTRACT

Respiratory diseases are one of the leading causes of death and disability in the world. Integration of AI with existing Chest X-Ray (CXR) diagnostics is currently a hot research topic. On similar lines, we propose a technique termed “Swasta-shwasa” for multi-class classification that associates CXR with one among Tuberculosis, COVID-19, Viral pneumonia, Bacteria Pneumonia, Normal and Lung Opacity ailments based on Deep Learning. The proposed technique which has accomplished an overall 98% test accuracy, 0.9991 AUROC, average Specificity of 99.82% and average Sensitivity of 98.51% involves four stages: Pre-processing, Segmentation, Classification and Saliency map visualization. Further, the trained model is used to predict on unseen real life data of COVID-19 cases from India and a cross-population generalization accuracy of 85% is witnessed. XAI is augmented for model interpretability. We also explore why CLAHE may not be suitable choice for pre-processing of CXRs.

Keywords: XAI, Healthcare, Deep Learning, COVID-19, Cross-population generalization, Respiratory Diseases, Chest X-Rays

1. INTRODUCTION

Importance to improve the healthcare infrastructure has increased exponentially ever since late 2019 with the outbreak of COVID-19 pandemic. On December 9, 2020 World Health Organization (WHO) Global Health Estimates revealed the leading causes of death and disability worldwide: 2000-2019. According to this report ¹, “The top global causes of death, in order of total number of lives lost, are associated with three broad topics: cardiovascular (ischaemic heart disease, stroke), respiratory (chronic obstructive pulmonary disease, lower respiratory infections) and neonatal conditions – which include birth asphyxia and birth trauma, neonatal sepsis and infections, and preterm birth complications.” Secondly, as indicated in Table 1, respiratory diseases are, significantly, detrimental to human lives next only to heart related diseases. However, respiratory diseases are, comparatively, more life-threatening diseases and could drive the patients into emergent situations as compared to heart related diseases. Few specific, factual information about lethal respiratory diseases are as follows:

- According to WHO², bacterial tuberculosis is the world's largest infectious killer, attacking 10 million people every year and killing 1.5 million people annually.
- Pneumonia can be caused by viruses, bacteria or fungi and is the leading cause of infectious child mortality worldwide, killing 808,694 children under 5 years of age in 2017³.
- The recent COVID-19, yet another respiratory disease, has resulted in a death toll of 4M in a span of nearly 2 years. Globally, as of July 23 2021, there have been 192,284,207 confirmed cases of COVID-19 reported to WHO⁴.

Table 1: Leading causes of death and disability worldwide: 2000-2019 (Source: WHO Global Health Estimates)

Top 10 global causes of death in 2019	Top 10 global causes of disability-adjusted life years (DALYs) in 2019
Ischaemic heart disease	Neonatal conditions
Stroke	Ischaemic heart disease
Chronic obstructive pulmonary disease	Stroke
Lower respiratory infections	Lower respiratory infections

¹<https://www.who.int/data/global-health-estimates>

²https://www.who.int/health-topics/tuberculosis#tab=tab_1

³<https://www.who.int/news-room/fact-sheets/detail/pneumonia>

⁴<https://covid19.who.int/>

Neonatal conditions	Diarrhoeal diseases
Trachea, bronchus, lung cancers	Road injury
Alzheimer disease and other dementias	Chronic obstructive pulmonary disease
Diarrhoeal diseases	Diabetes mellitus
Diabetes mellitus	Tuberculosis
Kidney diseases	Congenital anomalies

Whereas the earlier, non-contagious respiratory diseases have been handled with a sequence of diagnostics/medication by the healthcare ecosystem, efficiently, the recent addition of contagious disease, typically, the COVID-19 and its variants has brought in a sense of urgency with respect to diagnostics so as to ensure proper containment of the disease. As such, the normal course of diagnostics need be shortened and more reliable diagnostics need be conducted with minimal latency. Throat-swab (Reverse Transcription Polymerase Chain Reaction, RT-PCR) tests, Chest X-Rays (CXRs) followed by Computerized Tomography (CT) scans constitutes the normal sequence of diagnostics. The work reported in this paper suggests CXRs as a possible first step in the diagnostic process, solely, to accomplish a shortened time for diagnosis. The CXRs are preferred over CT Scan for the following and such other reasons:

- X-rays are cheaper and available in most of the health-care centres.
- CT scan is not preferred for contagious diseases like COVID-19 since the machine is big and needs to be cleaned after every scan.
- Invariably, it is suggested that CXRs are preferred over CT-Scan to avoid unnecessary exposure to radiation which might lead to cancer unless it is highly warranted to subject a patient to CT-scan.

Table 2 shows the features on CXR deciphered by the Radiologist.

Table 2: CXR features for the Respiratory related diseases

Disease	Features deciphered from CXRs by the Radiologist
TB	CXR demonstrates extensive patchy reticulonodular opacities, particularly on the left.
Bacterial pneumonia	CXR demonstrates airspace opacities with air bronchograms in the right lower zone
Viral pneumonia	CXR demonstrates diffuse irregular patchy inhomogeneous opacities in both lungs
COVID-19	CXR demonstrates bilateral air space patchy inhomogeneous opacities (consolidation), mainly distributed in the right lung and left lower lung zone.
Lung opacity	CXR demonstrates ill-defined opacity in left lingula region with loss of left heart border consistent with left lingula consolidation.

The main objective of this work is to build a Deep learning model which can identify these features with good explainability and strong correlation with the radiological findings, resulting in faster diagnosis, hence early treatment even in remote places.

Application of Deep Learning (DL) based multi-class classification for disease detection and classification is well researched for quite some time. Yujin Oh *et al.* [2] has proposed a local-patch based Deep Transfer Learning (DTL) model for classification into four classes: normal, tuberculosis (TB), bacterial pneumonia, and Viral pneumonia which includes the pneumonia caused by COVID-19 infection on limited dataset. Similarly, DTL has been studied in [3]–[5] with some modifications in the pre-processing stage. In [3], the original data is converted to neurosophic domain, [4] proposes to use Generative Adversarial Networks (GAN) to generate images in order to mitigate the overfitting problem as a result of limited dataset. Chithra *et al.* [6] has proposed an Adaptive Fractional Crow (AFC)-deep Convolution Neural Network (CNN) to classify and indicate the severity level of TB infection. In [7], authors have proposed a modified U-Net for segmentation followed by DTL-based classification of CXRs into Normal and TB.

Since this area has now become a hot-research topic, an in-depth literature survey has indicated that there are more than 200 research works which have been reported in the area of disease classification, specially, using the techniques of DL. However, most of these works have employed the conventional DL methodology that involves pre-processing, segmentation, classification and saliency map visualization. The research work reported in this paper attempts to study the Cross-population Generalizability of the model by testing on real life data which is also validated by human radiologist.

2. PROPOSED METHOD

The flowchart is as shown in Fig. 1. The Deep learning-based Classification of CXRs into Common lung pathologies (Bacterial pneumonia, COVID-19, Lung opacity, Normal, Tuberculosis, Viral Pneumonia) has four steps: Pre-processing, Segmentation, Classification and Saliency-map.

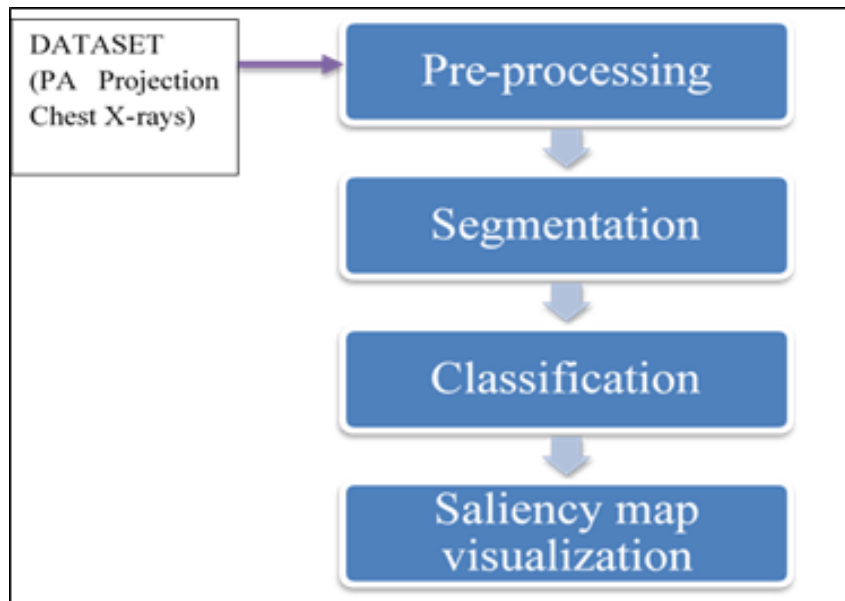


Figure 1: Flow Chart of the method

A. Pre-Processing Stage

This step removes the data heterogeneities and bias since the dataset is collected from different sources. This stage involves 2 steps: Histogram equalization to improve the contrast, followed by resizing to 150x150x3 since the number of neurons in the input layer of CNN is fixed.

Histogram equalization is a technique for adjusting image intensities to enhance global contrast of the image.

Let $\{x\}$ be a given image. Let n_i be the number of pixels having intensity i . The histogram of $\{x\}$ is the probability of an occurrence of a pixel of gray level i

$$p_x(i) = p(x = i) = \frac{n_i}{n} = \frac{\# \text{ of pixels with intensity } i}{\text{Total \# of pixels}} \quad \forall 0 < i < L \quad \text{---(I)}$$

The Cumulative Distribution Function (CDF) is defined as

$$cdf_x(i) = \sum_{j=0}^i p(x = j) \quad \text{---(II)}$$

Histogram equalization is a transformation function $y = T(x)$ which produces a new image $\{y\}$ with flat histogram and a linearized CDF across the value range, i.e.

$$cdf_y(i) = iK \quad \text{---(III)}$$

$$\text{Thus, } y = T(x) = cdf_x^{-1}(cdf_y(i)) \quad \text{---(IV)}$$

L is the total number of intensity values in the image and K is a constant in the range $[0, L-1]$.

B. Segmentation Network

Segmentation divides the image into different objects. Semantic segmentation classifies each pixel belonging to the same object as one class. By applying segmentation algorithm on pre-processed CXR, lung mask is obtained. The technique of Transfer Learning(TL) is used in this work: UNet-6v⁵ is adopted. UNet-6v is a supervised, fully convolutional network that uses pre-trained VGG-11 on the encoder path. Data augmentation, batch normalization, bilinear upscaling is used to boost the performance and the convergence speed. The Jaccard score is 0.9268 and Dice score is 0.9611. The output segmented image from the decoder path is a binary image of size 512 x 512 x 3.

C. Classification Network

The CNN based supervised classifier operates on the lung contour rather than the complete image. Each of the pixel corresponding to the lung area of the segmented image undergoes a logical inversion and gets bitwise-ANDed with the pre-processed image to obtain the lung contours. The CNN works on this dataset of lung contours of size 150 x 150 x 3 to carry out a 6-class classification. The 6-classes are Bacterial pneumonia, Lung opacity, Tuberculosis, Viral pneumonia, Covid-19 and Normal. The CNN Architecture designed for this work is as depicted in Fig. 2. The first part consists of 3 Convolution layers with 16,16,32 filters of size 3 x 3 respectively and stride = 1, followed by Batch normalization. The activation function used is Rectified Linear Unit (ReLU) and the window size for the Max pooling layer is set to 3 x 3. The Fully Connected layer consists of 1024 neurons followed by 6 neurons with Softmax activation function. Dropout layers, L2 Activity regularizer are used to reduce the model complexity and hence mitigate the overfitting problem.

⁵GitHub - IlliaOvcharenko/lung-segmentation: Lung segmentation for chest X-Ray images

```

Model: "sequential_1"
-----
Layer (type)                Output Shape                Param #
-----
conv2d (Conv2D)             (None, 150, 150, 16)      448
batch_normalization (Batch (None, 150, 150, 16)      64
max_pooling2d (MaxPooling2D) (None, 50, 50, 16)        0
dropout (Dropout)           (None, 50, 50, 16)        0
conv2d_1 (Conv2D)           (None, 48, 48, 16)        2320
batch_normalization_1 (Batch (None, 48, 48, 16)        64
max_pooling2d_1 (MaxPooling2 (None, 16, 16, 16)        0
dropout_1 (Dropout)         (None, 16, 16, 16)        0
conv2d_2 (Conv2D)           (None, 14, 14, 32)        4640
batch_normalization_2 (Batch (None, 14, 14, 32)        128
max_pooling2d_2 (MaxPooling2 (None, 4, 4, 32)         0
dropout_2 (Dropout)         (None, 4, 4, 32)         0
flatten (Flatten)           (None, 512)                0
dense (Dense)                (None, 1024)               525312
batch_normalization_3 (Batch (None, 1024)              4096
dropout_3 (Dropout)         (None, 1024)               0
visualized_layer0 (Dense)    (None, 6)                  6150
-----
Total params: 543,222
Trainable params: 541,046
Non-trainable params: 2,176
    
```

Figure 2: CNN Architecture designed

D. Saliency Map

In classification problems, being able to reason out the False-positive as well as False-negative is of paramount importance albeit, techniques/algorithms like RISE (Randomized Input Sampling for Explanation) [13] based on explanatory AI are sparingly used. In the present work, to validate the output of the CNN, RISE algorithm is employed. The RISE algorithm is model agnostic and generates a heat-map where the hotness indicates the contribution of each pixel to the CNN model's prediction (Fig 3). An excellent in-depth detail on explanatory AI is available in [14].

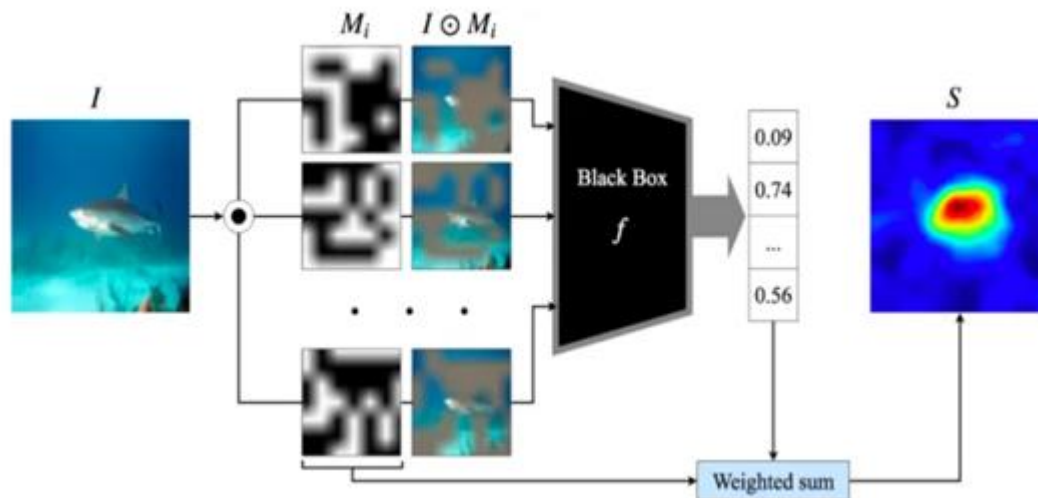


Figure 3: Overview of RISE [13]

3. DATASET

The training data set for the present research work is generated using three databases which provided raw Posteroanterior (PA) projection Chest X-ray images of patients suspected to be suffering from lung related ailments. The raw datasets used are as listed below:

- **Dataset - A:** Chest X-ray Images (Pneumonia) Database⁶ consists of CXRS belonging to Normal, bacterial and viral pneumonia combined.
 - **Dataset - B:** COVID-19 Radiography Database⁷ consists of Normal, Viral Pneumonia, COVID-19 and Lung Opacity ailments.
 - **Dataset - C: Tuberculosis Chest X-ray Database⁸ consists of Normal and Tuberculosis CXRs.**
- Dataset leveraged from these datasets are summarised in Table 3. The CXR images are manually cleaned by removing inappropriate images and validated by the Radiologist. The details of number of images before and after clean is also presented in Table 3.

4. EXPERIMENT AND RESULTS

A. Pre-Processing

Contrast Limited Adaptive Histogram Equalization (CLAHE) is a variant of adaptive histogram equalization which takes care of excessive enhancement of the contrast. CLAHE processes small areas in the image, known as tiles, not the entire image. This reduces the noise amplification due to global histogram equalization. Adjacent tiles are then combined using bilinear interpolation to eliminate artificial boundaries.

Table 3: Details of the dataset used in this work and distribution for train-test

Class name	No. of images		No. of images (6600 images Post – clean)	
	Before Clean	After clean	Training (90%)	Testing (10%)
Normal (No infection) [Dataset-A]	1341	11001	992	108
COVID-19 [Dataset-B]	3616	1100	987	113
Lung Opacity (Non-COVID lung infection) [Dataset-B]	6012	1100	982	118
Pneumonia (Bacteria + Viral) [Dataset-A]	3875	1100 (Bacteria Only)	983	117
Tuberculosis [Dataset-C]	3500	826 (Augmented to make 1100)	990	110
Viral Pneumonia [Dataset-B]	1345	1100	1006	94
Total (6 classes)	19689	6600	5940	660

Initially, CLAHE was used as part of pre-processing stage. But the CLAHE image was found to be not acceptable from the radiologist perspective since the clarity of the image is inordinately compromised. This remark from the radiologist is also evidenced in Fig. 4. This experimental observation, in fact, is supportive of the mathematical manifestation of histogram equalization summarized in Section 2. Whereas the linearity of the CDF is, experimentally, proved in the case of histogram equalized image Fig. 4(b), the CDF corresponding to CLAHE technique is found to follow the input image, smoothing out (linearizing) intermediate undulations (Fig. 4(c)) but fails to attain an overall linearization. In view of this observation, it is found that CLAHE technique which is highly prevalent in applications requiring local contrast enhancement becomes infeasible in the context of the present work.

B. Segmentation

The segmentation sample output is as illustrated in Fig. 5 in which Row 1 corresponds to Normal, Row 2 to Bacterial pneumonia, Row 3 to COVID-19, Row 4 to Lung opacity, Row 5 to TB and Row 6 to Viral pneumonia.

C. Training Details

The dataset consists of 1100 images/class * 6 classes = 6000 lung contours of size 150x150x3. This is randomly divided into 90% for training and 10% for testing and then normalized (Table 3, column 4-5).

Loss function: Categorical Cross-entropy

Optimizer: Adam

Learning rate: 0.001 (default)

Regularizer: L2 Activity Regularizer, l2 = 0.01 (default)

Epochs: 250

⁶<https://www.kaggle.com/paultimothymooney/chest-xray-pneumonia>

⁷<https://www.kaggle.com/tawsifurrahman/covid19-radiography-database>

⁸<https://www.kaggle.com/tawsifurrahman/tuberculosis-tb-chest-xray-dataset>

Batch size: 32

Training Platform: Google Colab, RAM = 13 GB, CPU.

Callback: model_checkpoint_callback i.e., save entire model each time when the validation accuracy has improved, in h5 format.

The best model was obtained at epoch =208 which gives a test accuracy of 98.48%.

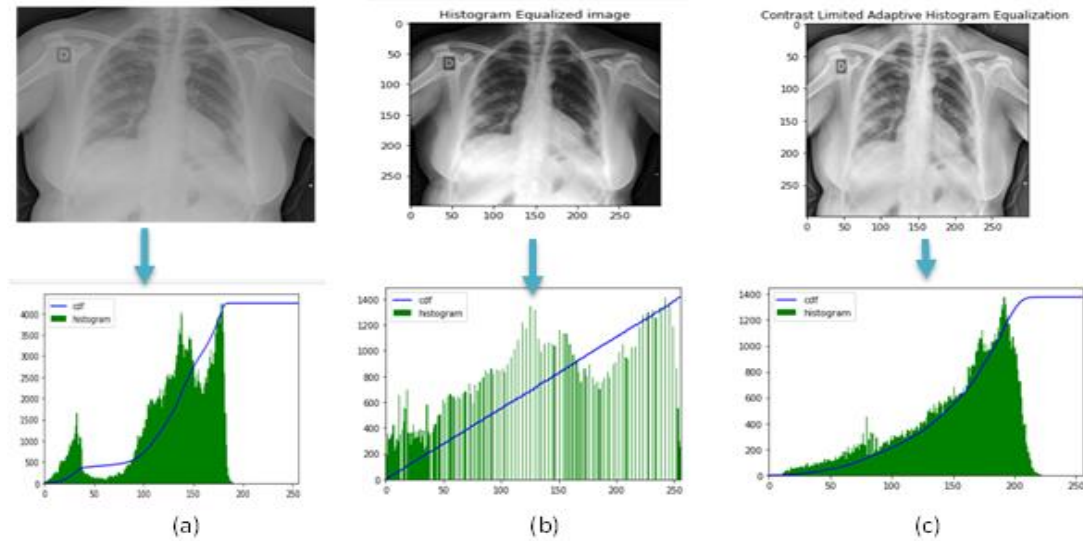


Figure 4: (a) Original Image (b) Histogram Equalized image (c) CLAHE image and their corresponding histograms and CDF

D. Classification Performance

The CNN designed is used for classification of CXRs into 6 classes namely Lung opacity, Normal, COVID-19, Tuberculosis, Bacteria and Viral Pneumonia. The best model achieves an overall validation accuracy of 98.48% on the unseen test data during training. The Kappa co-efficient is 98.2 and the average AUROC is 0.9991. However, for medical image analysis, more than accuracy, Positive predictive Value, Negative predictive value, Specificity etc. are considered more important. The results are tabulated in Table 5. The Confusion matrix, ROC Curve and Precision-Recall curves are shown in Fig. 6, Fig. 7, Fig. 8 respectively.

E. Cross-Population Generalizability

Cross-database or Cross-population generalizability demonstrates the diagnostic performance of the DL model on different population. As described in Section 3, for training and testing, CXRs from Dataset-A, Dataset-B and Dataset-C were used which did not have any CXRs of patients from India.

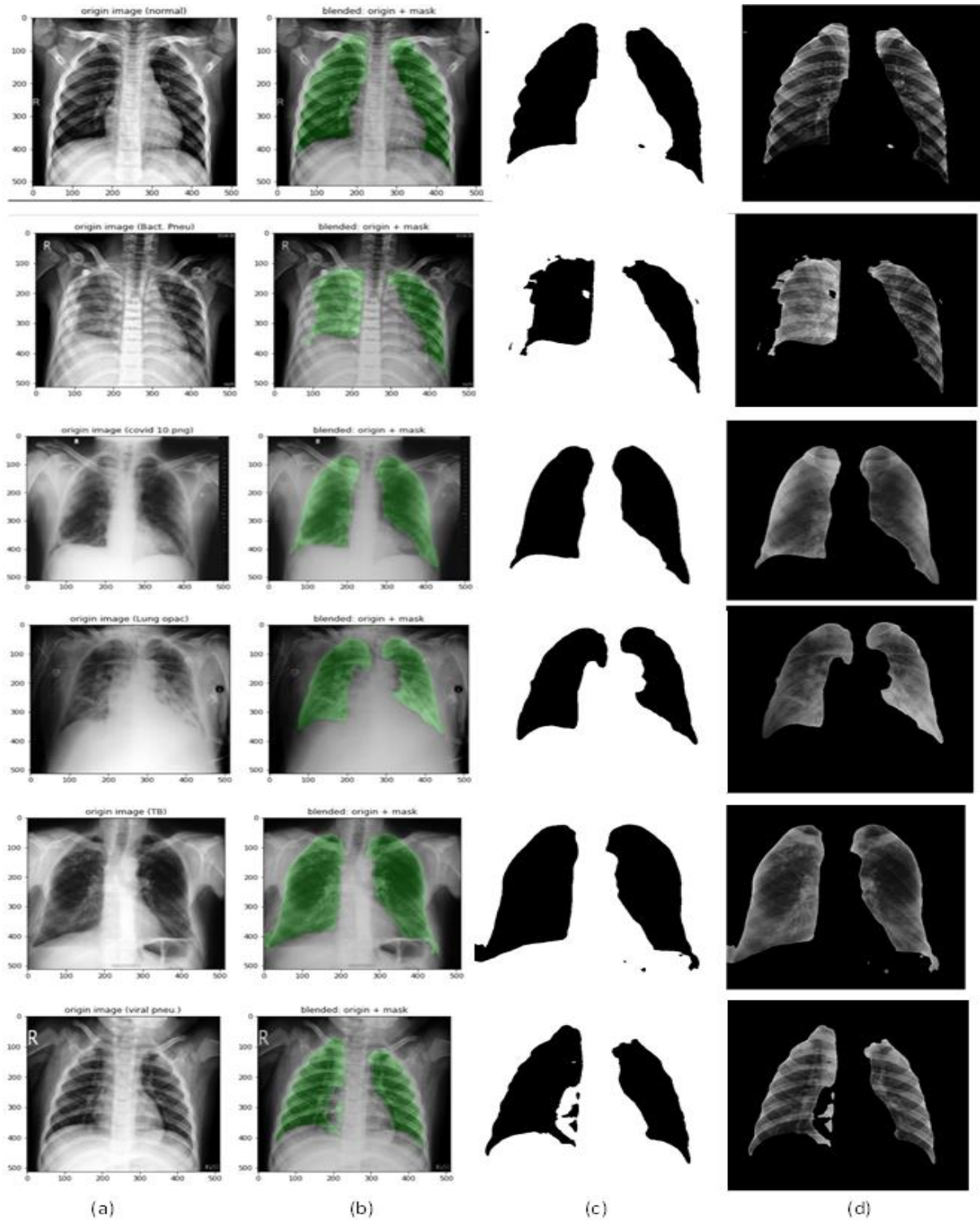


Figure 5: (a) Pre-processed image (b) Overlap of mask on (a) (c) Mask (d) Lung contour
 To check cross-database generalizability, CXRs belonging to the same lung ailments from India is used. The diagnostic performance of proposed model is summarized in Table 4.

Table 4: Cross-population Generalizability: Diagnostic performance

Class	No. of images	No. of images predicted correctly
Bacterial pneumonia	15	1
COVID-19	20	17
Lung opacity	15	0
Tuberculosis	18	0
Viral pneumonia	11	0

Except for COVID-19, the results from Table 4 strongly correlates with Seelwanet *al.* 's work [12], indicating that the diagnostic performance of AI model is specific to dataset, due to different technical specifications of CXR images and distribution of disease severity in different populations. Research is to be conducted in this direction further on how to overcome this problem and make AI for healthcare a reality irrespective of population.

F. Saliency Maps

Fig. 9 illustrates the saliency map for certain test input (Viral Pneumonia). The hotness indicates the weightage of the pixel in making the corresponding prediction. The prediction is Viral pneumonia and the saliency map partially correlates with the CXR features of the true class (Viral pneumonia). But, the saliency map has no or incorrect association with negative classes like Lung Opacity, COVID-19.

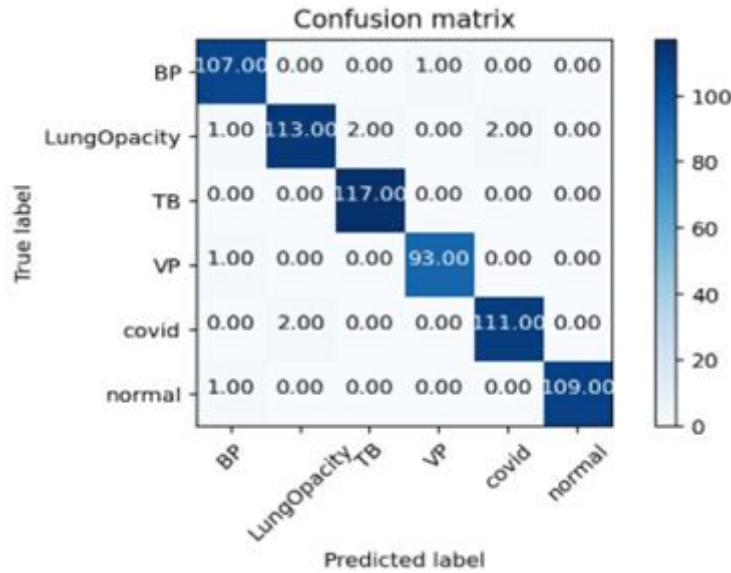


Figure 6: Confusion matrix
Table 5: Experimental Results

Class	Precision (PPV)	Recall (TPR, Sensitivity)	F1-score	Specificity (TNR)	NPV	AUROC	Classification accuracy
Bacterial Pneumonia	0.9907	0.9817	0.99	0.9982	0.9964	0.9999	0.9955
Lung opacity	0.9576	0.9826	0.97	0.9980	0.9963	0.9967	0.9894
TB	1.0000	0.9750	0.99	1.0000	0.9945	0.9998	0.9955
Viral Pneumonia	0.9894	0.9894	0.99	0.9982	0.9982	1.0000	0.9970
COVID-19	0.9823	0.9823	0.98	0.9963	0.9963	0.9985	0.9939
Normal	0.9909	1.000	1.00	0.9982	1.00	1.0000	0.9985
Micro-average	0.99	0.98	0.99	0.9982			
Macro average	0.99	0.99	0.99	-			
Weighted average	0.99	0.98	0.99	-			
Simple average	0.98	0.98	0.98	-	-	-	

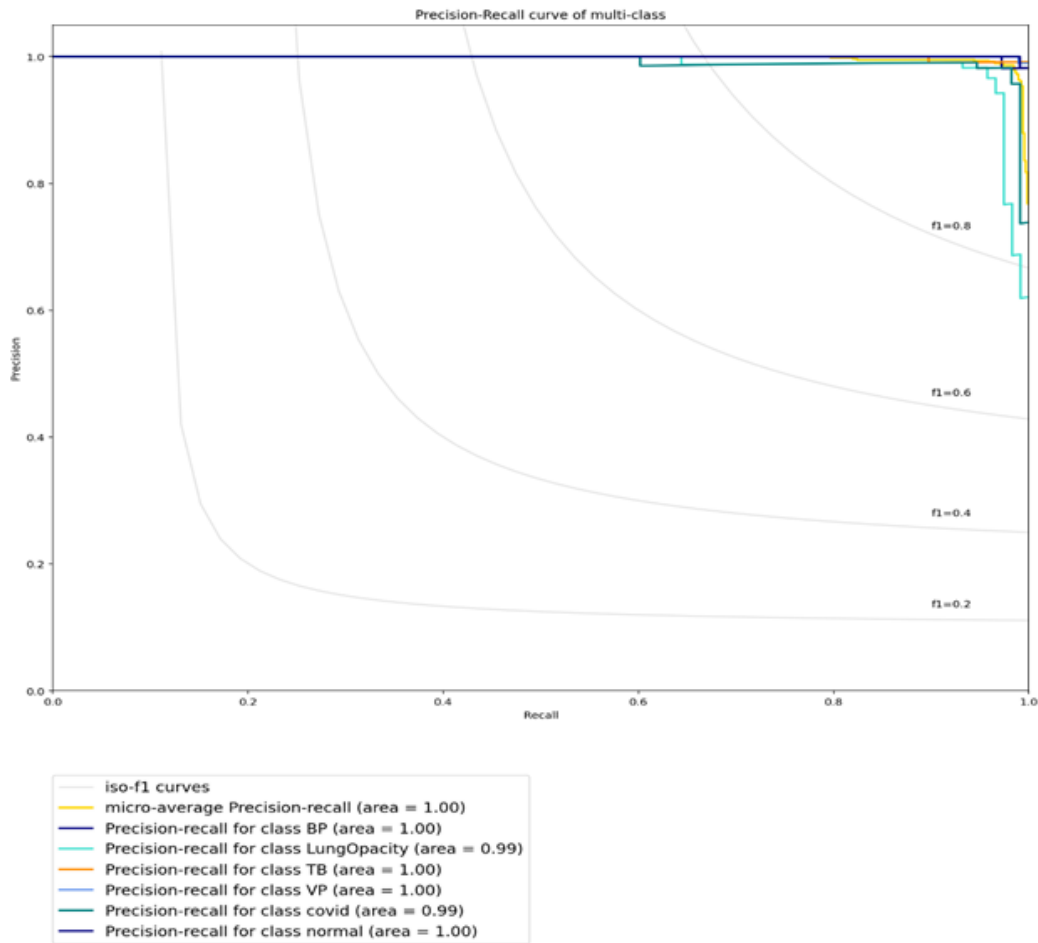


Figure 7: ROC Curve

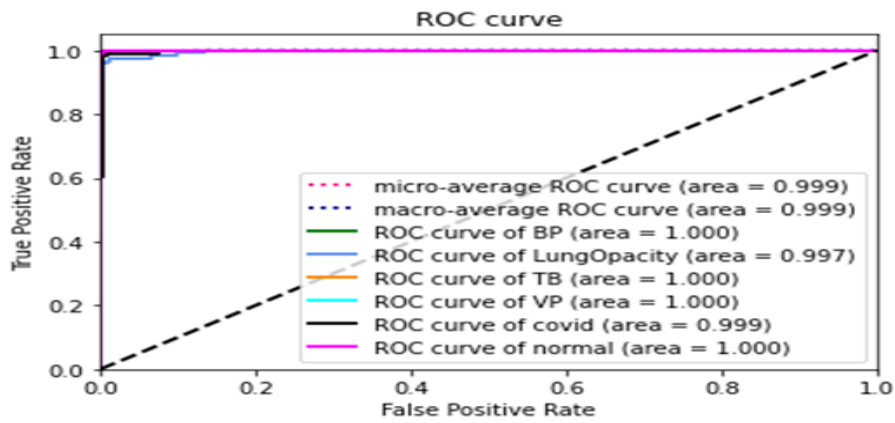


Figure 8: Precision -Recall curve

Actual: D:/DATA/contour/VP/8.png
 full pred [[0. 0. 0. 1. 0. 0.]]
 ['BP', 'LungOpacity', 'TB', 'VP', 'covid', 'normal']

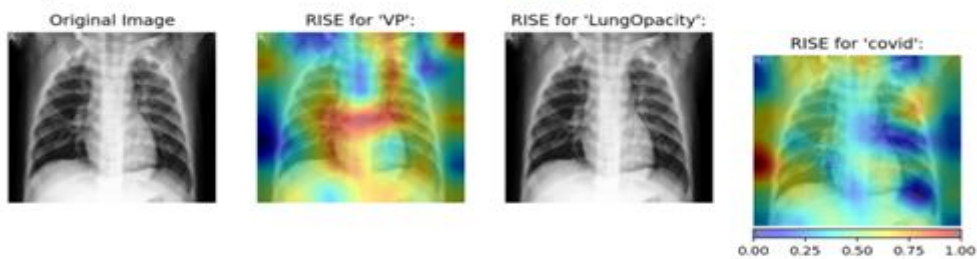


Figure 9: Saliency map on some test data

G. Comparison with Existing Literature

The comparison of proposed work with some of the recent works published in 2020 is given below. It is evident that the proposed methodology provides better metric-values comparatively with other existing techniques, indicating better performance. (Table 6)

Table-6:Comparison with existing literature

Author	Method and images	Evaluation metrics (%)
Yujin Oh et al. [2]	Random Local-patches with ResNet -18 4 classes (Normal: 191, TB:57, Bacterial pneumonia: 54, Covid-19 or Viral: 200)	Sensitivity: 85.9 Specificity:96.4 Accuracy: 88.9
Nour et al. [3]	Neutrosophic domain conversion + DTL 4 classes (Normal: 79, Bacterial pneumonia: 79, Viral Pneumonia: 79, Covid-19: 69)	Sensitivity: 87.5 Accuracy: 87.1
Chithraet al. [6]	AFC-deep CNN 3 classes (Normal: 25, TB with severity detection: 50)	Accuracy : 88 TPR: 82 FPR: 18
Tawasifuret al. [7]	Modified U-Net for segmentation + DTL 2 classes (Normal: 3500, TB: 700)	Accuracy: 98.4
Wang et al. [8]	COVID-Net using projection-expansion-projection-extension (PEPX) 3 classes (Normal:8066, Non-covid19 pneumonia: 5538, Covid-19: 358)	Accuracy: 93.3
Vishnu Madhan et al. [9]	X-CovNet : CNN 2 classes: 196 images for each class(Covid+, Covid-)	Accuracy: 98.4
Proposed method	CNN 6 classes : 1100 images each (Normal, TB, Bacterial pneumonia, Covid-19, Lung opacity, Viral pneumonia)	Sensitivity: 98.5 Specificity: 99.8 Accuracy : 98.5 Cohen Kappa: 98.2

5. CONCLUSION

A technique termed “Swastha-shwasa” for multi-class classification that associate CXR with one among Tuberculosis, COVID-19, Viral pneumonia, Bacteria Pneumonia, Normal and Lung Opacity ailments based on Deep Learning is implemented in this work. To the best of our knowledge, this is the first work to analyse the cross-population generalizability of the CNN model by predicting on real life data from India. We also recognize CLAHE may not be suitable algorithm in this context for pre-processing. The model achieves an overall 98% accuracy, 0.9991 AUROC, average Specificity of 99.82% and average Sensitivity of 98.51%. Despite good results, there are still some hindrances to deploy model in real-time due to the fact that the model is trained on a limited data and cross-population generalizability is achieved with only COVID-19 CXRs. Hence for future work, further research can be carried by employing Federated Learning which satisfies the data hungriness of the AI models while also preserving privacy on the patient’s information.

REFERENCES

1. X. Xie, Z. Zhong, W. Zhao, C. Zheng, F. Wang, and J. Liu, “Chest CT for typical 2019-ncov pneumonia: relationship to negative RT-PCR testing,” *Radiology*, p. 200343, 2020.
2. Y. Oh, S. Park and J. C. Ye, "Deep Learning COVID-19 Features on CXR Using Limited Training Data Sets", *IEEE Transactions on Medical Imaging*, vol. 39, no. 8, pp. 2688-2700, Aug. 2020, doi: 10.1109/TMI.2020.2993291.
3. Khalifa, N.E.M., Smarandache, F., Manogaran, G. et al. “A Study of the Neutrosophic Set Significance on Deep Transfer Learning Models: an Experimental Case on a Limited COVID-19 Chest X-ray Dataset”, *CognComput* (2021). <https://doi.org/10.1007/s12559-020-09802-9>
4. Mohamed Loey, FlorentinSmarandache and Nour E. M. Khalifa, "Within the Lack of Chest COVID-19 X-ray Dataset: A Novel Detection Model Based on GAN and Deep Transfer Learning" *Symmetry* 2020,12, no. 4: 651. <https://doi.org/10.3390/sym12040651>
5. Shervin Minaee, RaheleKafieh, Milan Sonka, Shakib Yazdani, GhazalehJamalipourSoufi, “Deep-COVID: Predicting COVID-19 from chest X-ray images using deep transfer learning”, *Medical Image Analysis*,2020, <https://doi.org/10.1016/j.media.2020.101794>
6. R . S. Chithra, P. Jagatheeswari, “ Severity detection and infection level identification of tuberculosis using deep learning”, *Int. Journal of Imaging Systems and Technology*, Wiley, April 2020, doi: <https://doi.org/10.1002/ima.22427>

7. T. Rahman et al., "Reliable Tuberculosis Detection Using Chest X-Ray with Deep Learning, Segmentation and Visualization," *IEEE Access*, vol. 8, pp. 191586-191601, 2020, doi: 10.1109/ACCESS.2020.3031384.
8. L. Wang and A. Wong, "COVID-net: A tailored deep convolutional neural network design for detection of COVID-19 cases from chest radiography images," *arXiv preprint arXiv:2003.09871*, 2020.
9. Madaan, V., Roy, A., Gupta, C. et al. , "XCOVNet: Chest X-ray Image Classification for COVID-19 Early Detection Using Convolutional Neural Networks", *New Gener. Comput.* (2021). <https://doi.org/10.1007/s00354-021-00121-7>
10. M.E.H. Chowdhury, T. Rahman, A. Khandakar, R. Mazhar, M.A. Kadir, Z.B. Mahbub, K.R. Islam, M.S. Khan, A. Iqbal, N. Al-Emadi, M.B.I. Reaz, M. T. Islam, "Can AI help in screening Viral and COVID-19 pneumonia?" *IEEE Access*, Vol. 8, 2020, pp. 132665 - 132676.
11. Rahman, T., Khandakar, A., Qiblawey, Y., Tahir, A., Kiranyaz, S., Kashem, S.B.A., Islam, M.T., Maadeed, S.A., Zughair, S.M., Khan, M.S. and Chowdhury, M.E., 2020. Exploring the Effect of Image Enhancement Techniques on COVID-19 Detection using Chest X-ray Images. *arXiv preprint arXiv:2012.02238*.
12. SeelwanSathitratanacheewin and Krit Pongpirul, "Deep Learning for Automated Classification of Tuberculosis-Related Chest X-Ray: Dataset Specificity Limits Diagnostic Performance Generalizability", *ScienceDirect*, August 2020. <https://doi.org/10.1016/j.heliyon.2020.e04614>,
13. Vitali Petsiuk, Abir Das and Kate Saenko, "RISE: Randomized Input Sampling for Explanation of Black-box Models", *British Machine Vision Conference (BMVC)*, 2018. Available [Online] <http://bmvc2018.org/contents/papers/1064.pdf>
14. Molnar, C. (2018). *Interpretable Machine Learning*. Retrieved from <https://christophm.github.io/interpretable-ml-book/>